AIAA Journal

VOLUME 2 MARCH 1964 NUMBER 3

Hypersonic Wakes and Trails

LESTER LEES*
California Institute of Technology, Pasadena, Calif

The distribution of observables in hypersonic wakes and trails is the result of a complex interaction of body shape, chemical kinetics, and the onset of laminar-turbulent transition This paper discusses progress and problems in these three areas with emphasis on scaling laws In the "near wake" the growth of the turbulent core and the cooling rate depend strongly on body shape The growth of the turbulent far wake is described by the universal relation $Y_{Tf}/(C_DA)^{1/2} \sim [x/(C_DA)^{1/2}]^{1/3}$ regardless of body shape or Reynolds number An analysis of data on laminar-turbulent transition in the wake of blunt bodies obtained in a wind tunnel and in a ballistic range shows that these data are correlated by taking a constant value of $(Re_{x\,f})_t = 5\,6 \times 10_4 \pm 15\%$ over a Mach number range from 3 6 to 14 4. (Here x is distance from the body to the location of transition) The minimum critical Reynolds number for a blunt body is about 5×10^4 at $M_\infty = 20$, based on freestream conditions and body diameter This value corresponds to an altitude of 220,000 ft for a body 6 ft in diameter For a sharp-nosed slender body, transition in the wake should appear at about the same altitude A tentative explanation of transition in hypersonic wakes is presented based on recent work on the instability of laminar compressible wakes Scaling parameters for oxygen-electron attachment and electron-ion recombination are derived, and theoretical calculations are compared with some recent experimental results For full-scale re-entry vehicles, oxygen-electron attachment in the wake is important below an altitude of about 150,000 ft This paper concludes with a brief discussion of some of the main problems for future research in this challenging field

Nomenclature

a = sound speed
A = area
c = phase velocity of laminar disturbance
$\bar{c}_g$ = dimensionless group velocity
c_I = $c_I^*/(u_f - u_0)$
c_R = dimensionless phase velocity of laminar disturbance in moving-fluid coordinates
c_S = dimensionless phase velocity of laminar disturbance in body-centered coordinates
C_D = total drag coefficient
C_{D_f} = turbulent inner-wake drag coefficient
d = body diameter
h = static enthalpy
L = length
M = Mach number
M_R = relative Mach number $(u_f - u_0)/a_f$
n = particle number density
n = electrons/cm^3
p = pressure
R_B = body base radius
R_N = body nose radius
Re = Reynolds number
s = distance along streamline
$\bar{s}$ = (s/d)
t = time
T = temperature
u = axial velocity component
Δu = $(u_f - u_0)$
x = axial coordinate
y = radial coordinate
$\bar{Y}$ = Howarth-Dorodnitsyn coordinate
α = $\alpha^* L$
α^* = wave number
$\alpha^* c_I^*$ = amplification rate
γ = ratio of specific heats
δ^* = displacement thickness
$\tilde{\epsilon}_T$ = effective turbulent diffusivity

Presented as Preprint 2662-62 at the ARS 17th Annual Meeting and Space Flight Exposition, Los Angeles, Calif, November 13–18, 1962; revision received December 16, 1963 This paper was prepared under the sponsorship and with the financial support of the U S Army Research Office and the Advanced Research Projects Agency, Contract No DA-04-495-ORD 3231; this research is a part of Project DEFENDER sponsored by the Advanced Research Projects Agency The author would like to express his appreciation to his colleagues A Demetriades and H Gold of the California Institute of Technology, and to A Hammitt and L Hromas of Space Technology Laboratories, Inc for their assistance in the preparation of this paper, under U S Air Force Ballistic Systems Division Contract No AF 04(694)-1

* Professor of Aeronautics, Firestone Flight Sciences Laboratory; also Consultant, Space Technology Laboratories, Inc

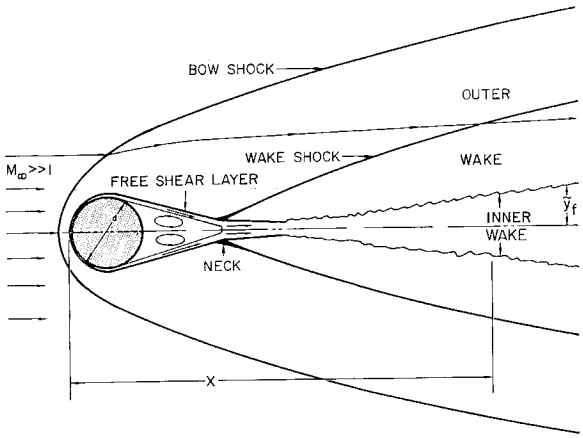

Fig 1 Wake behind blunt body at hypersonic speeds

ρ = density
ν = kinematic viscosity

Subscripts

e = local external inviscid
f = turbulent front
i = initial
I = outer inviscid
0 = along axis
T = turbulent
TR = transition
∞ = freestream

1 Introduction: Present Status of the Problem

EVERY body moving through a fluid medium leaves a characteristic signature in its wake At hypersonic speeds in a gas, electrons and radiating species are generated by the bow shock wave in front of a blunt body, and also by the deceleration and heating of the gas at the "neck" formed behind the body by the coalescence of the free shear layers shed from the body surface[1 2] (Fig 1) The nose shock produced by a sharp-nosed, unyawed slender body heats the gas only moderately, but significant concentrations of electrons and radiating species can be generated by viscous heating in the boundary layer over the surface and by compression at the "neck" (Fig 2) These species are swept into the wake, and are responsible for observable effects up to distances of hundreds or even thousands of body diameters behind the body

When the flow in the wake is entirely laminar and in thermodynamic equilibrium, the diffusion process is described in terms of well-known scaling laws,[3 4] and the problem is relatively straightforward † However, recent experimental studies[7 8] of wakes behind spheres and cylinders at hypersonic speeds show that transition to turbulent flow occurs in the viscous "inner wake" downstream of the neck if the Reynolds number exceeds a certain critical value (Fig 1) On the basis of these experiments, this critical Reynolds number based on conditions ahead of the body is about 5×10^4 at a velocity of the order of 20,000 fps, corresponding to an altitude of about 200,000 ft for a blunt body with a nose diameter of 1 ft Slattery,[9] Demetriades and Behrens,[10] and Pallone et al [11] have observed a similar phenomenon in wakes behind sharp-nosed bodies at hypersonic speeds Thus, any realistic model of the wake must allow for turbulent diffusion above the critical Reynolds number

At present the treatment of the turbulent wake is necessarily semiempirical [2 4] Turbulent diffusion is much faster than laminar diffusion, and the turbulent "front" spreads outward, engulfing the fluid originally contained in the outer wake (Fig 1) At each station the turbulent flow is assumed to behave like a "slice" of a low-speed, self-similar turbulent wake in Townsend's[12] sense In this model, the turbulence intensity at each station is proportional to the local value of the velocity difference $\Delta u = u_f - u_0$ across the inner wake, and the scale is proportional to the "proper" local wake width In fact, the effective turbulent diffusivity $\tilde{\epsilon}_T$ is represented by the expression‡

$$\tilde{\epsilon}_T = K \Delta u \tilde{Y}_{T_f}$$

where, for a body of revolution,

$$\tilde{Y}_{T_f}^2 = 2 \int_0^{y_f} \left(\frac{\rho}{\rho_f} \right) y dy$$

and K is inversely proportional to Townsend's "universal" Reynolds number Thus,[2]

$$\rho_f / \rho_\infty [\tilde{\epsilon}_T / u_\infty (C_D A)^{1/2}] \tilde{Y}_{T_f} \sim K \{ [C_{D_f}(\tilde{x}) / C_D] \}$$

where

$$\tilde{Y}_{T_f} = \bar{Y}_{T_f} (C_D A)^{-1/2} \qquad \tilde{x} = x (C_D A)^{-1/2}$$

C_D is the usual total body drag coefficient, and C_{D_f} is the local value of the drag coefficient corresponding to the momentum defect relative to the velocity u_f, already swallowed by the inner wake up to that station [At the neck, $(C_{D_f})_i \ll C_D$] The wake growth may be roughly described by means of the relation

$$\tilde{Y}_{T_f}(\tilde{x}) \sim \left[K \tilde{x} \frac{C_{D_f}(\tilde{Y}_{T_f})}{C_D} \right]^{1/3} \tag{1}$$

The development of the turbulent "near wake," and especially the enthalpy decay rate, depends strongly on body shape, because of its influence on the shape of the nose shock and the manner in which the momentum defect $C_{D_f}(\tilde{Y}_{T_f})$ is distributed across the outer wake (Sec 2) However, when $\tilde{x} \cong 1000$ practically all of the body drag has been swallowed by the turbulent inner wake, and beyond this region $\tilde{Y}_{T_f} \sim (K\tilde{x})^{1/3}$ regardless of the body shape or the Reynolds number

For thermodynamic equilibrium (for example) the decay of the peak enthalpy $h(0)$ along the wake axis is obtained by combining Eq (1) with the energy conservation integral across the inner wake, which takes the simple form

$$\frac{\rho_f}{\rho_\infty} \left(\frac{h(0) - h_f}{h_\infty} \right) \tilde{Y}_{T_f}^2 = \frac{(\gamma_\infty - 1) M_\infty^2}{4\pi G_2} \left(\frac{C_{D_f}(\tilde{Y}_{T_f})}{C_D} \right) \tag{2}$$

where

$$G_2 = \int_0^1 \left(\frac{h - h_f}{h_\infty} \right) \zeta d\zeta \qquad \zeta = \frac{\bar{Y}}{\bar{Y}_{T_f}}$$

(For a parabolic enthalpy profile, $G_2 = \frac{1}{4}$) If the body is blunt and the flow is in thermodynamic equilibrium, the inner wake is surrounded initially by hot gas $[(h_f/h_\infty) \gg 1]$, and the characteristic cooling distance is quite long even with turbulent diffusion [2] For example, for a sphere at a flight velocity of 22,000 fps, the equilibrium enthalpy on the wake axis is still about 25 times ambient at $x \cong 300$ and 10 times ambient at $x \cong 600$ At an altitude of 100,000 ft the peak electron density is about $2 \times 10^9/\text{cm}^3$ at $x \cong 300$, corresponding to the critical plasma frequency at uhf (400 Mc/sec) When the body is slender and sharp-nosed, or only slightly blunted, the inner wake is surrounded by relatively cool gas, and the temperature history along the axis is quite different; this case is examined in Sec 2

At low ambient density or high altitude, the flow field at hypersonic speeds is far from chemical equilibrium, and chemical and electronic rate processes play an important

† The effect of the pressure drop along the wake axis in the first 50–100 body diameters can be included in the analysis along the lines developed by Kubota[5] and Gold [6]

‡ In Ref 2 the symbol $Y_{T_f} = \bar{Y}_{T_f}/d$

role in determining the "initial" radial distributions of physical quantities in a transverse plane at the "neck," and the subsequent history of observables in the wake For blunt bodies, Gibson[13] and Hall, Eschenroeder, and Marrone[14] have shown that the "slow" three-body chemical recombination processes can be neglected altogether in the vicinity of the nose of the body if the ambient density is low enough In Fig 3 the thermodynamic regimes for a blunt body based on Gibson's work are indicated schematically To the left of the solid line the flow near the nose is in chemical equilib rium To the right of the dashed line chemical recombination near the body can be ignored, and the normalized physical quantities and mass fractions of chemical species are correlated by means of the binary scaling parameter $k_1\rho_\infty d/\mathfrak{M}_{ai}\, u_\infty \sim \rho_\infty d$ at a given flight velocity (Here k_1 is a representative dissociation rate "constant" in cm³/sec, and $\mathfrak{M}_{ai}$ is the weight of a molecule of air in grams) In this regime the atom and molecule mass fractions are "frozen" in the inviscid expansion region, but the frozen levels may lie well below infinite-rate equilibrium values calculated just behind the bow shock Dissociation is "self-limiting" because the temperature drops rapidly along a streamline in the shock layer as dissociation progresses; finally, the temperature drop caused by the expansion around the body effectively quenches the process [13 14]

At flight velocities less than 23,000 fps, electrons and ions play virtually no role in determining the temperature of the gas, and their local "environment" is dictated by the behavior of the atoms and molecules To the right of the dashed line in Fig 3 electron production can be ignored in the expansion region around a blunt body However, electron-ion recombination rates are much faster than chemical recombination rates, and must be taken into account The most important electron removal process near the body is the dissociative recombination

$$NO^+ + e^- \rightarrow N + O$$

Thus, one expects binary scaling to apply to the electrons even when electron-ion recombination is included The history of electron number density along a streamline is obtained by integrating the number density conservation equation

$$\rho(d/dt)(n/\rho) = -\alpha n^2 \qquad (3)$$

where $\alpha(T)$ is the rate "constant" in cm³/sec One obtains

$$\left(\frac{1}{n\,d}\right) - \frac{(\tilde\rho_i/\tilde\rho)}{(n\,d)_i} = \left(\frac{1}{u_\infty\tilde\rho}\right)\int_{\tilde s_i}^{\tilde s}\left(\frac{\alpha\tilde\rho}{\tilde u}\right)d\tilde s \qquad (4)$$

$\rightarrow$ expansion $\leftarrow$ $\leftarrow$recombination $\rightarrow$

where $\tilde s = s/d$, $\tilde\rho = \rho/\rho_\infty$, $\tilde u = u/u_\infty$, s is the distance along a streamline, and "i" denotes the location of electron production "cut-off" on the particular streamline When the flow field is characterized by the binary scaling parameter $\rho_\infty d$,

$$n\,d = f[\tilde s;\ \rho_\infty d\ \ (n\,d)_i]$$

at a given flight velocity

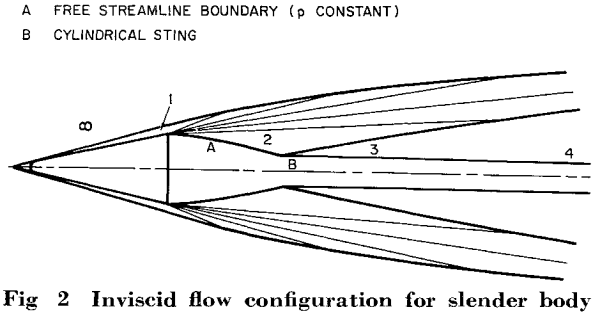

Fig 2 Inviscid flow configuration for slender body

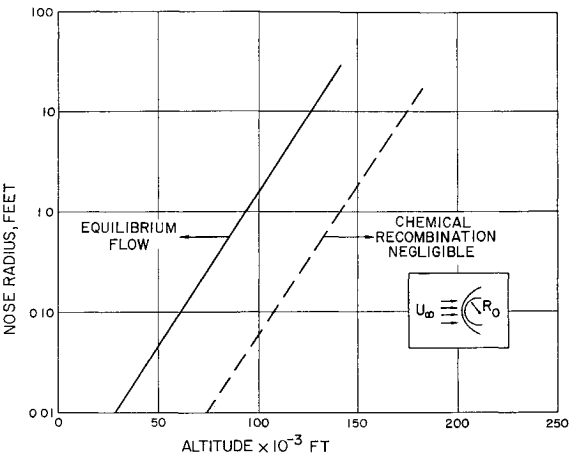

Fig 3 Thermodynamic regimes for hypersonic flow over a blunt body

To take some representative values, at a flight velocity of 23,000 fps the right-hand side of Eq (4) is of the order of 3×10^{-13} cm² at $\tilde s = 1$, whereas $(n)_i$ along a streamline that crosses the "strong" portion of the bow shock is about 5×10^{14}/cm³ at an altitude of 150,000 ft [13] Also, $(\tilde\rho_i/\tilde\rho)_{\tilde s=1} \cong 10$ Even for a body as small as 1 cm in diameter, electron-ion recombination is dominant The value of $n\,d$ at $s \cong 1$ is virtually independent of its initial value and is of the order of 3×10^{12}/cm² if d is in centimeters At an altitude of 150,000 ft the initial electron density n_i along a streamline that crosses a weaker portion of the bow shock (shock angle = 30°, $u_n = u_\infty \sin\theta_s = 11{,}500$ fps) is about 5×10^{10}/cm³ at "cut-off "[4] In that case electron-ion recombination is negligible compared to expansion in the flow around the body, even for $d = 100$ cm, and $n = 5 \times 10^9$/cm³ at $s \cong 1$ for all $d \leqq 100$ cm at this altitude

Chemical recombination in the inviscid flow behind a full-scale blunt body is not important above an altitude of about 150,000 ft; "swallowing" by the inner viscous core occurs first Below this altitude chemical recombination in the inviscid portion of the wake can no longer be ignored, and some attempts have been made to follow the progress of the various reactions by means of a streamtube approximation [15] In the laminar portion of the viscous core, diffusion is so slow that chemical recombination is much faster by comparison[16] when $Re_{f\,d} > 10^4$ ($h \geqq 250{,}000$ ft) Turbulent diffusion, on the other hand, is much faster than chemical recombination at altitudes above 150,000 ft The chemically reacting turbulent wake below this altitude has been treated[17–19] by an extension of methods employed in Refs 2 and 4 In Ref 19, for example, a separate conservation integral across the wake is written for each species, and, in addition, the continuity equation for each species is satisfied along the wake axis

If the atom mass fractions in the inviscid flow are virtually frozen, the inner wake behind a blunt body is surrounded by cool gas, and the temperatures in the turbulent wake drop very rapidly along the axis In this case the ionization rate is negligible, and electron-ion recombination or removal by oxygen attachment proceeds almost independently of the behavior of the chemical species, except for the effect of these species on the temperature The distribution of drag or momentum defect $C_{D_f}(\tilde Y_{T_f})$ across the outer wake is not much changed by chemistry, and so the wake growth $\tilde Y_{T_f}(\tilde x)$ and the swallowing rate are not much affected

The chief difficulty with these reacting viscous wake calculations is the lack of knowledge of the flow field in the "neck" region (Figs 1 and 2), which determines the "initial" conditions This difficulty is particularly acute for a sharp-nosed slender body Rates of production of chemical species and electrons are quite sensitive to the temperature in the

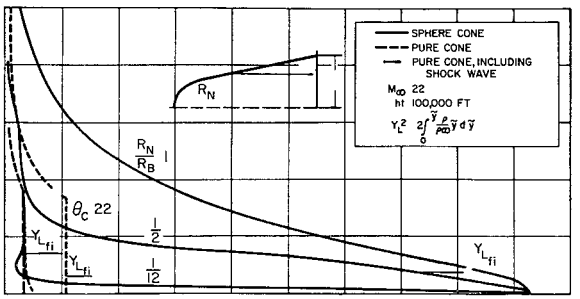

Fig 4 Inviscid equilibrium enthalpy profiles

neck region This temperature, in turn, depends on the velocity along the "dividing streamline" in the free shear layer, including the effect of the finite boundary-layer thickness at separation (Sec 5)

This brief discussion of hypersonic wakes and trails shows that the distribution of observables in the wake is the result of a complex interaction of body shape, rate chemistry, and the onset of laminar-turbulent transition In this paper we discuss some of the main aspects of these three elements in more detail, with emphasis on scaling laws whenever possible In Sec 2 the contrast between turbulent wakes behind sharp-nosed slender bodies and blunt bodies is brought out, and the effect of nose blunting on a slender body is examined A correlation of recent experimental results on laminar-turbulent transition in wakes is discussed in Sec 3, and some tentative theoretical explanations offered In Sec 4 we give a brief, approximate treatment of the problem of diffusion and recombination or oxygen attachment of electrons in a nonequilibrium turbulent wake, and compare our calculations with some recent experimental results on the decay of electrons in the wake behind a blunt body Finally,

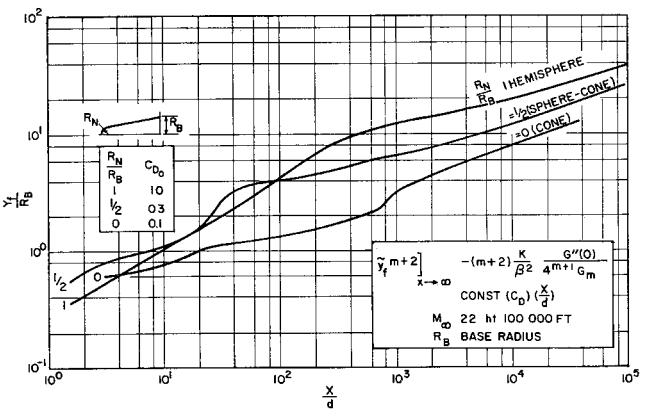

Fig 5a Effect of nose bluntness on growth of turbulent wake, physical coordinates

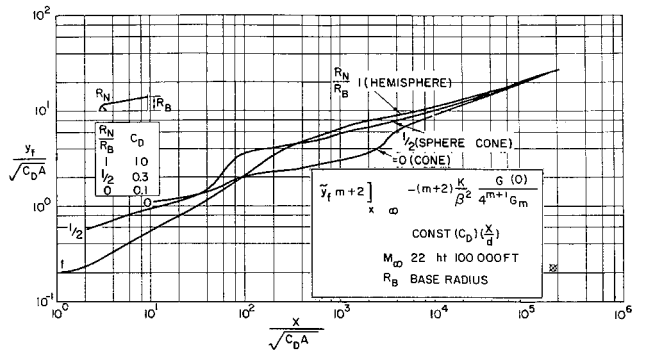

Fig 5b Effect of nose bluntness on growth of turbulent wake, "reduced" coordinates

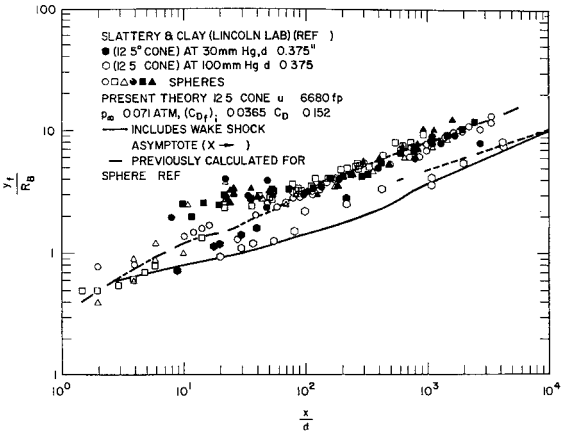

Fig 6 Comparison of theory and experiment on turbulent wake width

Sec 5 outlines some of the main difficulties and problems for future research in this fascinating field

2 Effect of Body Shape on Equilibrium Turbulent Wakes

According to the semiempirical description of turbulent wakes[2] the growth of the turbulent core in thermodynamic equilibrium depends on the enthalpy and the radial enthalpy gradient in the outer, inviscid flow at the location of the turbulent "front" Two interesting questions are explored with the aid of this model: 1) the contrast between the turbulent wakes for a blunt body and a sharp-nosed slender body, and 2) character of the "near-wake" for two bodies of different shape but the same C_DA

The approximate relations for wake growth and enthalpy decay given by Eqs (1) and (2) are helpful in understanding the results obtained by means of a detailed analysis [20] The drag coefficient C_{D_f} appearing in these relations is expressed in terms of the integral of the radial enthalpy profile as follows[2]:

$$\frac{C_{D_f}(\tilde{Y}_{L_f})}{C_D} = \frac{(C_{D_f})_i}{C_D} + \frac{4\pi}{(\gamma_\infty - 1)M_\infty^2}\int_0^{\tilde{Y}_{L_f}} \left(\frac{h}{h_\infty} - \frac{h_f}{h_\infty}\right)_L \tilde{Y}_L d\tilde{Y}_L \tag{5}$$

where

$$\tilde{Y}_L = \bar{Y}_L(C_DA)^{-1/2}$$

and§

$$\bar{Y}_L^2 = 2\int_0^y \left(\frac{\rho_L}{\rho_\infty}\right) y dy \tag{6}$$

Figure 4¶ shows the inviscid enthalpy distributions at a flight velocity of 22,070 fps and an altitude of 100,000 ft for a family of spherecones with a common half-angle of 12° and ratios of nose radius to base radius (R_N/R_B) of 0, $\frac{1}{12}$, $\frac{1}{2}$, and 1 (hemisphere) Also shown in this figure is the enthalpy distribution for a sharp-nosed cone with a half-angle of 22° having the same C_DA as the 12° cone with $R_N/R_B = \frac{1}{2}$ These distributions are obtained by calculating the shock shapes by the method of characteristics, and then expanding the flow isentropically to ambient pressure [20] The expansion around the blunt base is calculated by assuming that the static pressure is constant along the free streamline A

§ The turbulent and laminar mass flow quantities $\tilde{Y}_{T_f}$ and $\tilde{Y}_{L_f}$, respectively, are connected by the relation[2] $(\rho_f/\rho_\infty)\tilde{Y}_{T_f}^2 = \tilde{Y}_{L_f}^2 - \delta$ (constant)

¶ Figure 4 follows the notation of Ref 2, namely, $Y_L = \bar{Y}_L/d$, $\bar{y} = y/d$

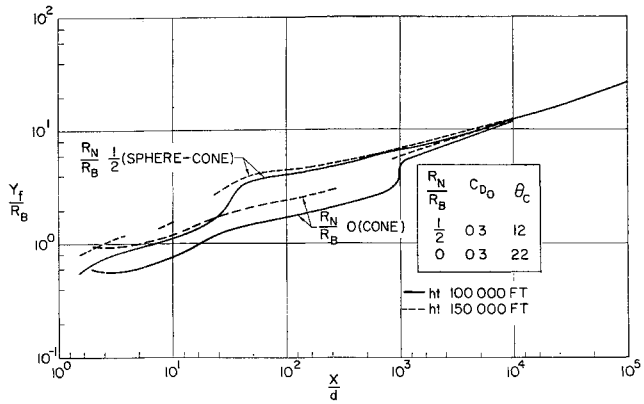

Fig 7 Growth of turbulent wake for a blunt-nosed and a sharp-nosed body with the same C_DA

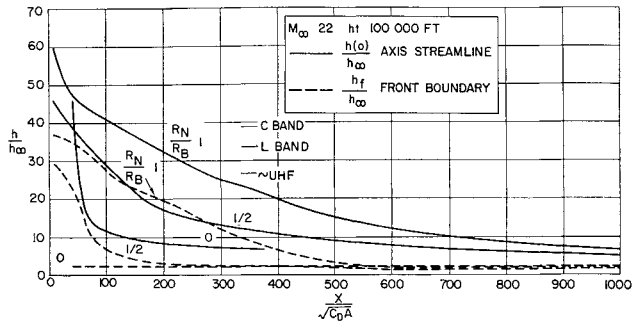

Fig 8 Equilibrium enthalpy distribution along wake axis and turbulent front

in Fig 2, and that the flow direction along this streamline is parallel to the wake axis just behind the wake shock ** At this velocity the wake shock itself has only a small effect on the enthalpy distribution (Fig 4)

Clearly, the extent to which the enthalpy distributions for the moderately blunted ($R_N/R_B = \frac{1}{2}$) and sharp-nosed cones differ depends on the amount of the enthalpy pulse near the axis which is absorbed by the viscous inner wake at the "neck" The boundaries of the inner wake are indicated on Fig 4 by the horizontal lines labeled $(Y_{Lf})_i$ These values of $(Y_{Lf})_i$ can be calculated from Eq (2) once $(C_{Df})_i$ and $(h_0/h_\infty)_i$ are known; $(h_0)_i$ is the enthalpy obtained when the velocity along the dividing streamline[21-23] is brought to rest isoenergetically, and $(C_{Df})_i$ is estimated from the friction and base pressure drags

Because the nose shock for the sharp-nosed cone is uniform in strength until it is intercepted by the expansion waves from the base (Fig 2), the enthalpy distribution is flat near the wake axis Of course the peak enthalpy is much lower than the peak enthalpy for a moderately blunted cone Suppose that the radial enthalpy profile for the sharp-nosed cone is represented by three straight-line segments, as follows:

$$(h_L/h_\infty) = (h_L/h_\infty)_0 \text{ when } 0 \leqq \tilde{Y}_L \leqq (\tilde{Y}_L)_1 \quad \text{(i)}$$

$$(h_L/h_\infty) = (h_L/h_\infty)_0 - a[\tilde{Y}_L - (\tilde{Y}_L)_1] \text{ when } (\tilde{Y}_L)_1 \leqq \tilde{Y}_L \leqq (\tilde{Y}_L)_2 \quad \text{(ii)}$$

where

$$a = [(h_L/h_\infty)_0 - 1][(\tilde{Y}_L)_2 - (\tilde{Y}_L)_1]^{-1}$$

$$(h_L/h_\infty) = 1 \text{ when } \tilde{Y}_L > (_L)_2 \quad \text{(iii)}$$

Then [Eq (5)]

$$C_{Df}/C_D = C_{D_{f_i}}/C_D \text{ when } \tilde{Y}_{Lf} < (\tilde{Y}_L)_1 \quad \text{(7a)}$$

$$C_{Df}/C_D = (C_{D_{f_i}}/C_D) + (\tfrac{2}{3})[\pi a/(\gamma_\infty - 1)M_\infty^2][\tilde{Y}_{Lf}^3 - (\tilde{Y}_L)_1^3] \text{ when } (\tilde{Y}_L)_1 < \tilde{Y}_{Lf} < (\tilde{Y}_L)_2 \quad \text{(7b)}$$

and, of course,

$$C_{Df} = C_D \text{ when } \tilde{Y}_{Lf} > (\tilde{Y}_L)_2 \quad \text{(7c)}$$

Thus, Eqs (1) and (7) predict that the turbulent core behind a sharp-nosed cone grows slowly in the near-wake region, until the turbulent "front" reaches $(\tilde{Y}_L)_1$, after which an explosive growth occurs over a relatively short distance Once the front passes $\tilde{Y}_{L_2}$ the wake takes up its asymptotic far-wake behavior For the moderately blunted cone, on the other hand, the radial enthalpy gradient is large near the axis (Fig 4, $R_N/R_B = \frac{1}{2}$), and one expects the turbulent core to grow rapidly in the near wake as soon as swallowing commences

These qualitative predictions are borne out by the results of the detailed calculations of wake growth (Figs 5a and 5b) Experimental results obtained by Slattery and Clay[9] show similar trends (Fig 6) In Fig 7 we compare the growth of the turbulent core for two bodies of different shape, but with the same C_DA: 1) blunt-nosed cone with $\theta_c = 12°$, and $(R_N/R_B) = \frac{1}{2}$; and 2) sharp-nosed cone with $\theta_c = 22°$ Evidently the difference in near-wake growth for these two bodies depends to some extent on the Reynolds number through $(C_{Df})_i$; of course the far wakes are identical

Even more striking is the contrast between the decay of peak enthalpy along the axis for the sharp-nosed and blunt-nosed cones The sharp cone entrains gas more slowly, but the gas absorbed is relatively cool As predicted by Eqs (2) and (7) the peak enthalpy drops rapidly with distance behind the body (Fig 8); the peak enthalpy is 10 times ambient at $\tilde{x} \cong 150$, as compared with a corresponding distance of $\tilde{x} \cong 700$ for the hemisphere Because the equilibrium electron density is so sensitive to temperature, the decay in peak electron density is quite marked even for the moderately blunted cone (Fig 9) Also shown for comparison are the curves for pure diffusion of a "foreign" material for the sharp cone and the hemisphere; as expected,

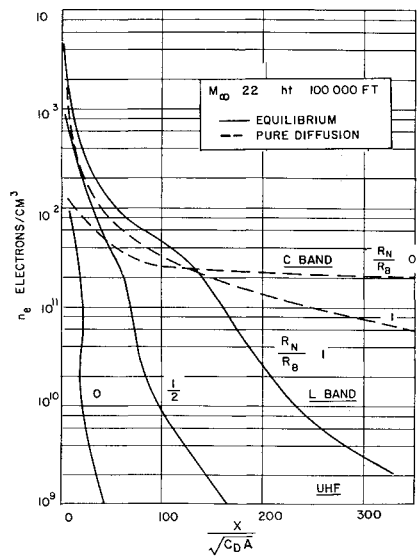

Fig 9 Effect of nose bluntness on equilibrium electron density along wake axis

** For the hemisphere and the blunted cones, the flow is determined by setting p_3/p_2 (Fig 2) equal to the pressure ratio obtained by an isentropic compression of the velocity along the dividing streamline [21-23] For the sharp-nosed cones, p_3 is close to ambient pressure, and its value was estimated $\cong 1\,2p_\infty$

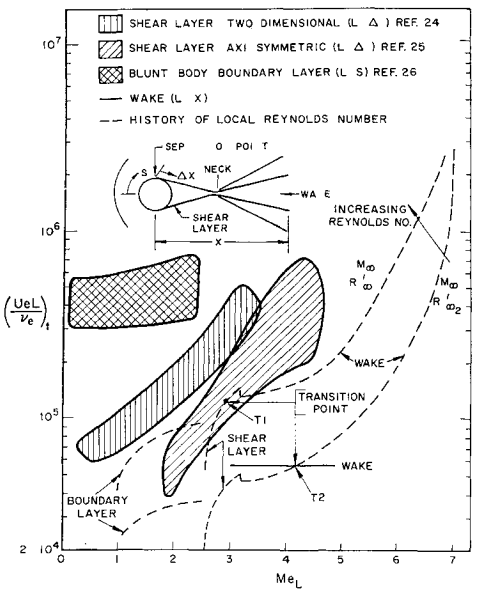

Fig 10 Local transition Reynolds number vs local Mach number

the peak concentration decays slowly in the near wake of a sharp cone because of the relatively slow rate of entrainment The diffusion rate increases once swallowing of the radial enthalpy gradient begins (Figs 5a and 5b) Except at low altitudes, the electronco ncentration in the wake is actually far from equilibrium, and the rate of decay of electron density is governed by the combined effect of diffusion and recombination or oxygen attachment (Sec 4)

3 Laminar-Turbulent Transition in Hypersonic Wakes

When the boundary layer on the body is laminar, laminar-turbulent transition occurs (if at all) in the downstream flow regions with the highest velocity gradients These regions are the free shear layers (or annulus) shed from the body surface, and the viscous inner wake downstream of the "neck" (Fig 1) Three different questions arise: 1) what is the origin of laminar-turbulent transition in these regions?; 2) what is the "proper" Reynolds number governing the location of transition when it does occur?; and 3) what is the "proper" minimum Reynolds number below which turbulent flow in the wake cannot be maintained?

Experimental studies[24 25] show that a laminar free shear layer is remarkably stable when the local velocity at the outer edge of the layer is supersonic In Fig 10 the observed transition Reynolds number $(Re_L)_{TR} = (u L/\nu)_{TR}$ for a laminar shear layer based on fluid properties at the outer edge and the length of laminar "run" is plotted as a function of local Mach number For a blunt body at hypersonic speeds $M \cong 2\,5$ in equilibrium flow, and $(Re_L)_{TR} = 10^5$; for nonequilibrium flow $M \cong 3\,5$–$4\,0$, and $(Re_L)_{TR} \cong 2 \times 10^5$ For a sharp-nosed cone with a half-angle of 12°, $M \cong 15$ at a flight number of 20, and $(Re_L)_{TR}$ is no lower than 10^6 ††

This important property of the laminar free shear layer is certainly in the direction predicted by Lin[27] on the basis of the small disturbance theory of laminar stability, provided that one accepts the hypothesis that only subsonic disturbances are important for stability [28 29] In order for such disturbances to exist in the mixing region between two parallel streams, the phase velocity c must be subsonic with respect to the mean flow in both streams Thus,

$$u_1 - c < a_1 \quad \text{and} \quad c - u_2 < a_2 \quad \text{where} \quad u_1 > u_2$$

By adding these two inequalities one obtains the relation

$$u_1 - u_2 < a_1 + a_2 \tag{8}$$

In the case of the free shear layer behind a body $u_2 \cong 0$, a_2 is the sound speed in the recirculating region just behind the body, and $u_1 = u$, $a_1 = a$, so that Eq (8) becomes $M < 1 + (a_0/a)$ If $a_0 = a$ the condition for the existence of subsonic disturbances is $M < 2$, whereas if the temperature in the recirculating region is equal to the stagnation temperature this condition is $M_e < 2\,5$ When the local Mach number exceeds these values subsonic disturbances are impossible, and the laminar flow is stable to small perturbations Starting from a different point of view, Landau[30] reached similar conclusions in his analysis of the stability of a sharp discontinuity between two parallel streams

Downstream of the neck the relative velocity $(u_f - u_0)$ governs the stability of the inner viscous wake and not u_f [Here u_f and u_0 are the velocities at the edge and center of the inner wake, respectively] Subsonic disturbances must satisfy the condition $u_f - c < a_f$, or

$$-c_R = (u_f - c)/(u_f - u_0) < (1/M_R) \tag{9}$$

where c and c_R are the phase velocities of the disturbance in body-centered and moving fluid (u_f) coordinates, respectively, and $M_R = (u_f - u_0)/a_f$ is the "proper" relative Mach number According to the laminar wake flow solutions, $[(u_f - u_0)/u_f] \sim (x)^{-(m+1)/2}$ where $m = 0$ for two-dimensional flow and $m = 1$ for axisymmetric flow Thus, even when the "external" flow (u_f) is hypersonic M_R be comes subsonic eventually, and Eq (9) can always be satisfied far enough downstream of the neck The location along the wake axis at which neutral or self-excited subsonic disturbances first become possible is determined by the permissible values of the phase velocity c_R given by laminar stability theory, together with Eq (9) ‡‡

Gold[32] has extended the analysis of Batchelor and Gill[33] for the inviscid stability of axisymmetric, incompressible laminar jets to the more general problem of compressible wakes and jets He finds that the necessary and sufficient condition for the existence of neutral or "adjacent" self-excited subsonic disturbances is that for some value of $w = [(u_f - u)/(u_f - u_0)] = w$, the gradient of the product of density and vorticity in a certain direction should vanish §§ When this condition is satisfied the phase velocity of the neutral disturbance is given by

$$-c_R = w = f[(T_0 - T_f)/T_f]$$

Gold[32] shows that two-dimensional compressible wakes are generally dynamically unstable In axisymmetric compressible wakes the axisymmetric disturbance mode ($n = 0$) exists only under special conditions, but the "sinuous" ($n = 1$) mode is almost always unstable

Numerical calculations[32] of the dependence of $-c_R$ on $[(T_0 - T_f)/T_f]$ have been carried out for the antisymmetric two-dimensional disturbance ¶¶ For example, near the neck in the wake of a blunt body at hypersonic speeds $(T_0 - T_f)/T_f \cong 0\,5$, and Gold finds that $-c_R = 0\,5$ According to Eq (9) M_R must be less than 2 0 Now $u_0 \ll u_f$ near

†† For comparison the transition Reynolds numbers on a highly cooled blunt body observed by Stetson[26] are also indicated on Fig 10

‡‡ In Ref 31 the criterion $M_R < 2$ was used provisionally to obtain rough stability estimates

§§ In a two-dimensional wake this direction is normal to the plane of the flow; in an axisymmetric wake this direction is tangential to the helix of constant phase [32]

¶¶ Calculations for axisymmetric disturbances are now in progress, but the results for $-c_R$ are not expected to differ greatly from the two-dimensional case

the neck and $M_R \cong M_f \cong 2.5$, for a blunt body Thus the wake goes unstable not far downstream of the neck For a slender body at $M_\infty = 20$, $M_f \cong 10$, and $[(T_0 - T_f)/T_f] = 6$ near the neck In this case $-c_R \cong 0.1$, and according to Eq (9) the wake is unstable not far from the neck Thus, at hypersonic speeds one expects laminar-turbulent transition to occur in the near-wake region for both blunt and slender bodies, but the actual location of transition depends on the amplification rates of the unstable disturbances The "sinuous" mode has recently been observed preceding transition in schlieren and shadowgraph photographs of the near-wake behind a slender cone at hypersonic speeds [11, 32]

It is not surprising that transition in the inner wake should be governed by a Reynolds number based on local rather than "freestream" properties, but it is somewhat startling that the location of transition is determined by a constant value of $(Re_{x\,f})_{TR}$ independent of body diameter In Fig 11a the observed location of transition x_{TR}/d in the wakes behind cylinders and spheres at supersonic and hypersonic speeds is plotted against $(Re_{f\,d})^{-1}$ where $(Re_{f\,d})$ is the local Reynolds number based on body diameter and conditions at the edge of the inner viscous wake The Graduate Aeronautical Laboratory, California Institute of Technology (GALCIT) hypersonic wind-tunnel data[1, 8] represent a series of independent experiments at $M_\infty = 5.8$ using a hot wire anemometer, pitot and static pressure measurements, and helium and argon diffusion data, with cylinder diameters varying from 0.10 to 0.30 inch The sphere data was obtained by optical methods in the Massachusetts Institute of Technology Lincoln Laboratory[7, 9] free flight ballistic range, with sphere diameters varying from 0.125 to 0.500 inch at Mach numbers of 3.6, 7.2, 7.6, and 14.4 With a few exceptions the data is correlated over this entire range of parameters by the straight line $(Re_{x\,f})_{TR} = 5.6 \times 10^4 \pm 15\%$ At any given flight Mach number $p_\infty x_{TR} =$ constant [7, 9]

Tentatively, we conclude that transition in the wake of a blunt body at hypersonic speeds bears a close resemblance to the transition occurring at low speeds in the laminar wake behind a thin, flat plate set parallel to the flow [34] In our case the neck takes the place of the plate trailing edge According to the interesting experimental and theoretical investigation of Sato and Kuriki,[34] transition is initiated by a linear regime in which small, two-dimensional disturbances grow exponentially in the downstream direction The growth rates observed by Sato and Kuriki agree remarkably well with the calculated amplification rates given by laminar theory [32, 34] This region is followed by a nonlinear regime characterized by the development of a double row of vortices, which leads finally to the three-dimensional development of turbulence itself ***

In the linear regime the amplification ratio for an unstable disturbance of a given frequency is given by

$$\log\left(\frac{Q}{Q_i}\right) = \int_{x_i}^{x}\left[\frac{(\alpha^* c_I^*)}{c_g^*}\right] \tag{10}$$

where x_i is the station at which this frequency "goes unstable," $\alpha^* c_I^*$ is the local amplification rate, α^* is the wave number, and c_g^* is the group velocity Now $\alpha^* = (\alpha/L)$, where L is related to wake width, and $c_I^* = c_I(u_f - u_0)$, so that Eq (10) becomes

$$\log\left(\frac{Q}{Q_i}\right) = \int_{x_i}^{x}\left[\frac{\alpha c_I}{\bar{c}_g}\right]\left[\frac{u_f - u_0}{u_f}\right]\left(\frac{dx}{L}\right) \tag{11}$$

where

$$\bar{c}_g = 1 + [(u_f - u_0)/u_f][c_R + \alpha(\partial c_R/\partial\alpha)]$$

*** The growth of the rms fluctuations along the wake axis in the linear regime, followed by a gradual decay,[34] is strikingly similar to the hot-wire results obtained by Demetriades[8] in the cylinder wake at $M_\infty = 5.8$, and by Demetriades and Behrens[10] in the wakes behind slender wedges at $M_\infty = 6.0$

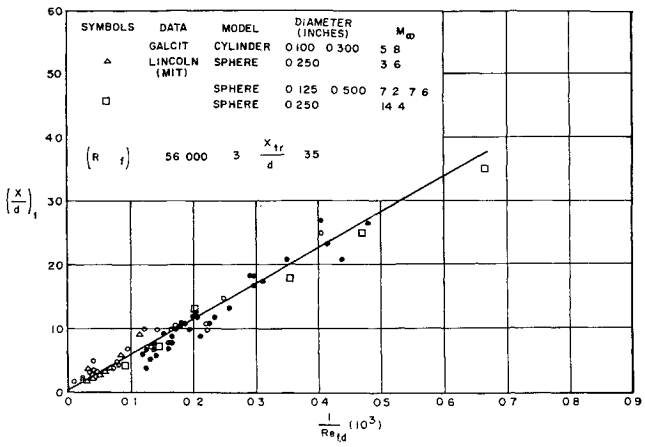

Fig 11a Correlation of transition in hypersonic wake behind blunt bodies

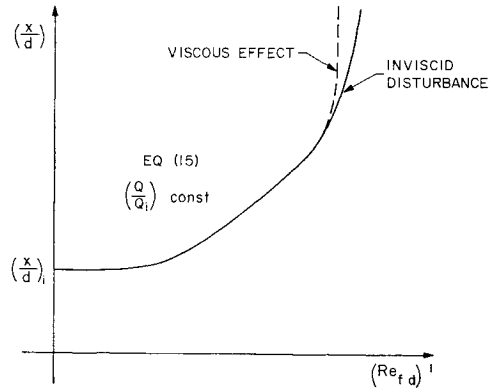

Fig 11b Distance required for fixed amplification ratio of unstable disturbance in wake (schematic)

Now for two-dimensional wakes[32]

$$[(u_f - u_0)/u_f](1/L) = (\rho_\infty/\rho_f)[(C_{D_f} Re_{f\,d})/8\pi^{1/2}](1/x) \tag{12}$$

where the appropriate drag coefficient is the value of $C_{D_f} = C_{D_{f_i}}$ in the inner laminar wake An approximate relation for this drag coefficient is[20]

$$(\rho_\infty/\rho_f)(C_{D_f})_i \cong 3/(Re_{f\,d})^{1/2} \tag{13}$$

By using this estimate of $(C_{D_f})_i$, Eq (11) becomes

$$\log\left(\frac{Q}{Q_i}\right) = \int_{(x_i/d)}^{(x/d)}\left[\frac{(\alpha c_I)}{c_g}\right]\left(\frac{3}{8\pi^{1/2}}\right)(Re_{f\,d})^{1/2} d\left(\log\frac{x}{d}\right) \tag{14}$$

But $(\alpha c_I/\bar{c}_g)$ corresponds to the "inviscid" amplification rate and is very nearly independent of (x/d), so that Eq (14) leads to the relation

$$(x/d) = (x_i/d)\quad (Q/Q_i)^N \tag{15}$$

where

$$N = (\bar{c}_g/\alpha c_I)(8\pi^{1/2}/3)[1/(Re_{f\,d})^{1/2}]$$

A schematic representation of Eq (15) for a fixed, arbitrary value of (Q/Q_i) is given in Fig 11b ††† At high Reynolds numbers laminar diffusion and wake growth are very slow, so the quantity $(u_f - u_0)/L$ in Eq (11) is nearly constant, and the unstable disturbances grow rapidly along the wake axis At low Reynolds numbers diffusion and wake growth are rapid, and the absolute amplification rate, which is

††† A representative value for a blunt body wake is $[\alpha c_I/\bar{c}_g] \cong 0.1$

proportional to $[(u_f - u_0)/u_f](1/L)$, is much lower; hence the nonlinear regime (and laminar-turbulent transition) moves downstream ‡‡‡ By some remarkable coincidence the intermediate portion of the curve of (x/d) vs $(Re_{f\,d})^{-1}$ is almost a straight line! However, it is not entirely clear why the slope of this line is so nearly the same in two-dimensional and axisymmetric blunt-body wakes

This provisional explanation is equally applicable to hypersonic wakes behind sharp-nosed slender bodies For example, an analysis[31] of the experimental results on wake transition obtained by Slattery[9] behind sharp-nosed cones at $M_\infty = 6$ gives $(Re_{x\,f})_{TR} \cong 2\,3 \times 10^5$ This value is surprisingly close to the value of $(Re_{x\,f})_{TR}$ found experimentally by Demetriades and Behrens[10] for a series of slender wedges in the GALCIT hypersonic wind tunnel at $M_\infty = 6$ The fact that the value of $(R_{x\,f})_{TR}$ for slender bodies at $M_\infty = 6$ is higher than for blunt-body wakes may be explained by the fact that the nondimensional amplification rate αc_I [Eqs (11) and (15)] decreases with increasing values of $(T_0 - T_f)/T_f$, or increasing M_f Recently Pallone et al [11] correlated their experimental wake transition data for slender cones obtained in the Avco/RAD Ballistic Range in terms of a plot of $(Re_{x,f})_{TR}$ vs $M_R \cong M_f$ up to flight Mach numbers of the order of 13

The location of transition in the wake moves downstream as the ambient pressure is reduced, but this aft movement of transition cannot continue indefinitely (see Fig 11b) Eventually a minimum critical Reynolds number is reached below which wake turbulence cannot maintain itself against the action of viscous dissipation Roughly speaking, this point is reached when the effective turbulent diffusivity $\tilde{\epsilon}_T$ falls below the appropriate laminar diffusivity For a two-dimensional blunt body the ratio of these two quantities is given by the relation[2]

$$\frac{(\tilde{\epsilon}_T/u_\infty d)}{(\nu_f/u_\infty d)} \cong 0\,015 C_{D_f} \left(\frac{\rho_\infty}{\rho_f}\right) Re_{f\,d} \sim Re_\theta \tag{16}$$

where θ is the momentum thickness Again the appropriate drag coefficient is not the total drag of the body, but the value of C_{D_f} in the inner laminar wake, which swallows momentum defect in the outer flow very slowly; thus, $C_{D_f} \cong (C_{D_f})_i$ Using the estimate of $(C_{D_f})_i$ given by Eq (13), Eq (16) becomes

$$(\tilde{\epsilon}_T/\nu_f) \cong 0\,045(Re_{f\,d})^{1/2} \tag{17}$$

and

$$(Re_{f\,d})_{\min} \cong 500$$

A similar analysis for the axially symmetric wake gives

$$\frac{\tilde{\epsilon}_T}{\nu_f} \cong 0\,02 \left(C_{D_f} \frac{\rho_\infty}{\rho_f}\right)^{1/2} \frac{(h_f/h_\infty)^{1/2}}{[(\gamma_\infty - 1)M_\infty{}^2]^{1/2}} \left[\frac{h_0 - h_f}{h_f}\right]^{1/2} Re_{f\,d} \tag{18a}$$

Using the estimated value of $(\rho_\infty/\rho_f)(C_{D_f})_i$ for a sphere,[20] one obtains

$$(\tilde{\epsilon}_T/\nu_f) \cong 0\,01(Re_{f\,d})^{3/4} \tag{18b}$$

from which

$$(Re_{f\,d})_{\text{mi}} \cong 500$$

The data of Kendall[35] and Behrens[50] on cylinders show that experimentally the actual value of $(Re_{f\,d})_{\text{mi}\ c}$ is about 1500 By combining this lower limit with a fixed value of $(Re_{x\,f})_{TR} = 5\,6 \times 10^4$ it follows that at hypersonic speeds transition in the wake of a blunt body cannot occur aft of $(x/d) \cong 40$

A similar analysis can be carried out for a sharp-nosed slender body, except that in this case $(h_0/h_f) \gg 1$, $(h_f/h_\infty) = 0(1)$, and the appropriate laminar diffusivity to be compared with $\tilde{\epsilon}_T$ is [31]

$$\bar{\nu} = \tfrac{1}{2}(\mu_f + \mu_0)/\tfrac{1}{2}(\rho_f + \rho_0) \cong (\mu_0/\rho_f)$$

One finds

$$(\tilde{\epsilon}_T/\bar{\nu}) = (0\,05/M_\infty)(Re_{f\,d})^{3/4} \tag{19}$$

At $M_\infty = 5$, $(Re_{f\,d})_{\min} \cong 500$ for a sharp-nosed slender body; at $M_\infty = 20$ $(Re_{f\,d})_{\min} \cong 3000$ Now the Reynolds number based on freestream or ambient fluid properties is given by $(Re_{\infty\,d}) = (\nu_f/\nu_\infty)(Re_{f\,d})$ Thus, at $M_\infty = 20$ the estimated minimum critical Reynolds number $(Re_{\infty\,d})_{\min}$ for a sharp-nosed slender body is about 3×10^4, applying the factor of 3 just noted, whereas $(Re_{\infty\,d})_{\text{mi}}$ for a blunt body is about 5×10^4

Summarizing, the tentative picture of transition in the wake at hypersonic speeds that emerges from this discussion is as follows: Below a certain minimum critical Reynolds number the wake is laminar Above this limit transition first appears about 40–50 diam behind the body if the body is blunt, and then moves forward as the ambient pressure increases, maintaining a constant value of $(Re_{x\,f})_{TR} = 5\,6 \times 10^4$, independent of body diameter When transition reaches the neck it gets "stuck" there until Re_L exceeds $(Re_L)_{TR}$ for the free shear layer; then it "jumps" to the free shear layer, and eventually appears in the boundary layer on the body (Fig 10) For a sharp-nosed slender body, transition first appears in the wake at lower ambient pressure and somewhat further back in terms of body diameter than for a blunt body, especially at lower hypersonic speeds Again transition moves rapidly forward as the ambient pressure increases but this forward motion slows down when the location of transition approaches the neck

When the value of $(Re_{f\,d})_{\min}$ for a blunt body is converted to ambient conditions, we estimate that $(Re_{d\,\infty})_{\min\ c} \cong 5 \times 10^4$ at $M_\infty = 20$ This minimum critical Reynolds number corresponds to an altitude of about 200,000 ft for a body 6 ft in diameter and agrees well with Lin's[36] meteor radar observations of a turbulent wake behind Col Glenn's capsule during re-entry at an altitude of 220,000 ft For a sharp-nosed slender body at $M_\infty = 20$ with the same base diameter, transition should appear in the wake at about the same altitude In fact the most remarkable aspect of the wake transition problem is the relative insensitivity of the location of transition (in body diameters) to body shape, size, and flight Mach number

4 Decay of Electron Density in Hypersonic Nonequilibrium Turbulent Wakes

4 1 Electron Removal Rates

When the electron density is high and the ambient gas density is low, the most important electron-removal process in air is the dissociative recombination discussed briefly in Sec 1, namely, $NO^+ + e^+ \rightarrow N + O$ In a hypothetical one-dimensional flow at constant density and constant velocity the electron clean-up rate by this mechanism is given by

$$(dn/dt) = \bar{u}(dn/dx) = -\alpha n^2 \tag{20}$$

where α is in cm³/sec According to Lin's[37] experimental results, $\alpha = (3 \times 10^{-3})T^{-3/2}$ Recent experimental studies[38] of electron-ion recombination in the Cornell Aeronautical Laboratory shock tunnel gave a rate constant "of the same order of magnitude" Figure 12 shows the history of electron decay by this process alone at $T = 1000°$K and $\bar{u} =$

‡‡‡ At very low Reynolds numbers viscous damping enters the problem, and the wake flow is stable below a certain minimum critical Reynolds number (see Fig 11b)

7×10^5 cm/sec, corresponding to conditions representative of hypersonic nonequilibrium turbulent wakes As Lin and Teare[15] pointed out, electrons disappear very rapidly when the electron density is high ($n \geq 10^{11}$/cm^3), and n soon takes on its "asymptotic" behavior given by $(1/n) = (\alpha x/u)$, independently of the initial level But when n drops below 10^{11}/cm^3, electron-ion recombination slows down [Eq (20)], and moderate but significant concentrations of electron density would persist for very large distances, if no other process intervened For example, Fig 12 shows that n_e drops below 10^8/cm^3 only after a distance of 700 m

At low or moderate electron densities and high ambient gas density, three-body electron-removal mechanisms are much faster than electron-ion recombination The most important three-body process for the turbulent wake is the affinity between electrons and molecular oxygen,§§§ represented by the reaction

$$O_2 + e^- + O_2 \rightarrow O_2^- + O_2 \qquad (21)$$

Here the additional oxygen molecule acts as a third body whose task is to take away the excess energy left over after the formation of O_2^- ¶¶¶ At constant density the electron clean-up rate by the forward reaction alone is given by

$$(dn/dt) = -Kn_{O_2}{}^2 n \qquad (22)$$

where K is measured in cm^6/sec The three-body attachment coefficient K [Eq (22)] was measured by Biondi et al[39] in pure oxygen at 300°K and in oxygen-helium mixtures containing 1–5% of oxygen at $T = 77$°K, over a range of electron energies from about 0 02 ev to 1 ev For thermal electrons at 300°K, $K \cong 2\,8 \times 10^{-30}$ cm^6/sec In the absence of experimental data at the temperatures of interest we assume that ****

$$K = (8\,4 \times 10^{-28}/T) \text{ cm}^6/\text{sec}$$

By using this expression for K, taking $n_{O2} = \frac{1}{5} n_{\text{ai}}$, and assuming constant temperature and flow velocity for purposes of illustration, Eq (22) is integrated to give

$$n = n_0 \exp\left(-\frac{3\,4 \times 10^{-29}}{T} \frac{n_{\text{air}}{}^2 x}{\bar{u}}\right) \qquad (23)$$

In Fig 12 this electron decay process at various altitudes is illustrated for $T = 1000$°K, $\bar{u} = 7 \times 10^5$ cm/sec, and $n_{\text{air}} = n_{\text{ambient}}$ (300/1000) (Clearly, the decay rate is quite sensitive to temperature at constant pressure, being proportional to T^{-3}) Above an altitude of 150,000 ft ($p_\infty = 1\,1$ mm Hg), oxygen attachment is unimportant, except as a "final" clean-up mechanism But the relaxation distance decreases like $n_{\text{air}}{}^{-2}$, and below an altitude of 120,000 ft ($p_\infty \cong 3\,5$ mm Hg) this process obviously must be taken into account, especially for $n_e < 10^8$–10^9

At temperatures above about 700°K the net electron clean-up rate by attachment is slowed down appreciably by the reverse of reaction (21), involving electron formation by collisional detachment If no other processes were involved these two reactions would reach equilibrium, and the relative concentrations of electrons and negative ions would be given by an expression of the form[40]

$$\frac{n_e}{n_{O_2^-}} = A \frac{T^{3/2}}{n} \exp\left(-\frac{\Delta E}{kT}\right) \qquad (24)$$

where A is a constant of order 10^{14}, n is gas density (no / cm^3), and ΔE is the molecular oxygen electron affinity; recent measurements[40] show that ΔE is equal to 0 46 ± 0 02 ev

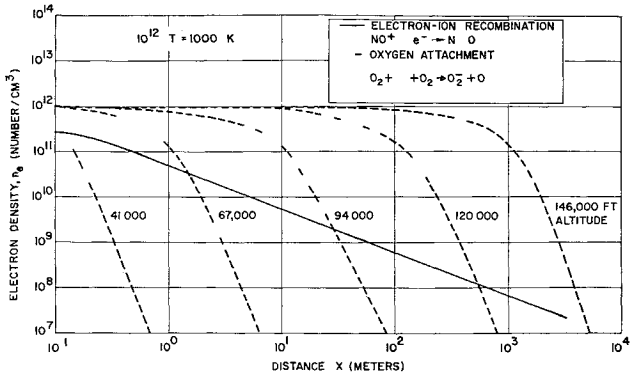

Fig 12 Comparison of electron removal rates

Negative molecular oxygen ions could be removed from the wake by mutual charge neutralization reactions, such as

$$NO^+ + O_2^- \rightarrow NO + O_2$$

or by the charge exchange reaction

$$O_2^- + O \rightarrow O_2 + O^- \qquad (25)$$

Generally $(n_O/n_{NO^+}) \gg 1$ (even though $n_O/n_{O_2} \ll 1$), and the second reaction is probably the more important one Unfortunately, the charge exchange activation energy is not known accurately, and recent calculations by Webb and Hromas[41] show that the removal rate of O_2^- is sensitive to the value assumed for this energy †††† In the absence of adequate information about charged particle reactions we may state that Eq (22) gives the fastest possible rate of removal of electrons by attachment, whereas Eq (24) leads to the slowest rate of removal In order to illustrate the combined effects of turbulent diffusion, electron-ion recombination, and oxygen attachment as simply as possible, we have selected reaction (21) to represent the attachment process

4 2 Diffusion and Electron Removal in a Turbulent Wake

In a steady two-dimensional or axially symmetric turbulent wake the continuity equation for any species in an effective binary mixture takes the following form:

$$\rho u(\partial K_i/\partial x) + \rho v(\partial K_i/\partial y) = \dot{w}_i + (1/y^m)(\partial/\partial y)[\rho \epsilon_M y^m (\partial K_i/\partial y)] \qquad (26)$$

where ϵ_M is the turbulent mass diffusivity, $\dot{w}_i = m_i(dn_i/dt)_P$ is the net production rate in g/cm^3/sec, and $K_i = n_i m_i/\rho$ is the mass fraction (Here $m = 0$ for two-dimensional flow and $m = 1$ for axially symmetric flows) By multiplying Eq (26) by y^m, integrating across the turbulent core, and using the over-all continuity equation, one obtains

$$\frac{d}{dx}\left[\int_0^{\bar{Y}_{T_f}} n_i u \frac{T}{T_f} \bar{Y}_T{}^m d\bar{Y}_T\right] = \left(\frac{n_i}{\rho}\right)_f \frac{d}{dx} \times \left[\rho_f \int_0^{\bar{Y}_{T_f}} u\, \bar{Y}_T{}^m d\bar{Y}_T\right] + \int_0^{Y_T} \left(\frac{dn_i}{dt}\right)_P \frac{T}{T_f} \bar{Y}_T{}^m\, dY_T \qquad (27)$$

For electrons,

$$(dn_e/dt)_p = -\alpha n_e{}^2 - \beta n_{\text{air}}{}^2 n_e \qquad (28)$$

if both electron-ion recombination and oxygen attachment

§§§ Because of rapid diffusion in a turbulent wake the atomic oxygen concentration is diluted, and O_2 plays the most important role in removing electrons by the formation of negative ions

¶¶¶ According to Chanin, Phelps, and Biondi,[39] N_2 is about 50 times less efficient than O_2 as a third body

**** More recent data[40] show that K is virtually independent of temperature in the range 300°K < T < 600°K

†††† The charge exchange activation energy ΔE_{CE} for the reverse of reaction (25) is estimated to lie between 1 and 1 5 ev Since the atomic oxygen electron affinity is about 1 5 ev, no activation energy is required for the forward reaction (25) if the lower estimate $\Delta E_{CE} = 1$ ev is chosen In that case this reaction is very efficient at temperatures below about 1000°K, and the forward reaction (21) proceeds unhindered [41]

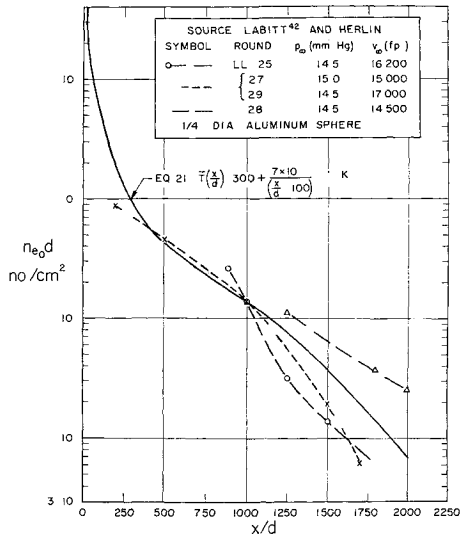

Fig 13 Decay of electron density in the nonequilibrium turbulent wake of a blunt body

are considered simultaneously; here $\alpha = 3 \times 10^{-3}/T^{3/2}$ and $\beta = 3\,4 \times 10^{-29}/T$ (Sec 4 1)

By analogy with the methods employed in the case of an equilibrium turbulent wake,[2] suppose that

$$n = n_0 F(\bar{Y}_T/\bar{Y}_{T_f}) \tag{29a}$$

and

$$(T_0 - T)/(T_0 - T_f) = G(\bar{Y}_T/\bar{Y}_{T_f}) \tag{29b}$$

where the subscript zero denotes properties on the wake axis Actual integration of Eq (27) must be carried out in conjunction with the energy integral equation for T/T_f and, possibly, one or two chemical species integral equations Such calculations have been programmed for an electronic computer by M Webb and L Hromas at Space Technology Laboratories and are now in progress

In order to bring out some of the main features of the electron density history in a rough way, we will make the following approximations: 1) electrons in the "outer" inviscid wake are neglected; i e , $(n)_f = 0$ in Eq (27); for a blunt body this restriction means that $\tilde{x} > 200$–300; 2) $u = \bar{u}$, a mean velocity; 3) $n = n_0 \exp(-\bar{Y}_T^2/\bar{Y}_{T_f}^2)$‡‡‡‡; and 4) the gas temperature is taken to be constant over a wake cross section, but the mean value varies with axial distance, i e , $T = \bar{T}(x)$

With the aid of these crude approximations and Eq (28), Eq (27) takes the following form for an axially symmetric wake:

$$(d/dx)(n_{e0}\bar{Y}_{T_f}^2) = -(\alpha/2\bar{u})n_0^2\bar{Y}_{T_f}^2 - (\bar{\beta}n_{a_i}^2/\bar{u})n_0\bar{Y}_{T_f}^2 \tag{30}$$

The integral of this equation is

$$\frac{1}{n_{e0}d} = \left(\frac{\bar{Y}_{T_f}^2}{\bar{Y}_{T_f}^2}\right)_N g(\xi)\left[\frac{1}{(n_0d)_N} + \int_{\xi_N}^{\xi}\frac{\alpha}{2\bar{u}}\frac{(\bar{Y}_{T_f}^2)_N}{(\bar{Y}_{T_f}^2)}\frac{d\xi'}{g(\xi')}\right] \tag{31}$$

where

$$g(\xi) = \exp\left[\int_{\xi_N}^{\xi}\left(\frac{\bar{\beta}n_{a_i}^2 d}{\bar{u}}\right)d\xi''\right] \tag{31a}$$

Here $\xi = x/d$, and N denotes values at the neck According to Eq (31a) the O_2-electron attachment parameter is

$$\lambda = \overline{\bar{\beta}n_{a_i}^2 d}/\bar{u} \tag{32}$$

‡‡‡‡ Note that integrations in Eq (27) now extend from 0 to ∞

where the bar denotes a suitably defined average value Then [Eq (31)],

$$n_0 d = f(\xi; (n_0 d)_N; \lambda)$$

When $\lambda\xi \ll 1$, oxygen attachment is unimportant and Eq (31) describes the combined effect of electron-ion recombination and wake spreading At a certain value of $\xi \sim 1/\lambda$ oxygen attachment makes its appearance, and by $\xi \sim 3/\lambda$ the electron density history in the wake is dominated by attachment plus wake spreading

In Fig 13 the rough description of electron density history in the wake given by Eq (31) is compared with experimental observations in a ballistic range behind a $\frac{1}{4}$-in -diam aluminum sphere made by Labitt and Herlin[42] (Massachusetts Institute of Technology Lincoln Laboratory), using a uhf cavity The flight velocities and ambient pressure for these four shots are indicated on the figure In carrying out the computations in Eq (31) the values of $\bar{Y}_{T_f}$ employed were taken to be identical with those calculated for the wake behind a sphere in equilibrium For a blunt body $(n\,d)_N \cong 3 \times 10^{12}$/cm^2 The variation of average temperature along the wake axis is approximated by the function $\bar{T}(x) = 300 + (7 \times 10^4)/[(x/d) + 1000]^{2/3}$ °K, so that $\bar{T} = 3530$°K at the neck, $\bar{T} = 1000$°K at $x/d = 900$, and $\bar{T} = 725$°K at $x/d = 2000$ For all four cases $p_{wake} \cong p_\infty = 15$ mm Hg, and

$$\frac{\bar{\beta}n_{a_{ir}}^2 d}{\bar{u}} = \frac{1\,39 \times 10^{-3}}{(\bar{T}/1000)^3} \qquad \frac{\alpha}{2\bar{u}} = \frac{10^{-13}}{(\bar{T}/1000)^{3/2}}\ \text{cm}^2$$

The effect of O_2-electron attachment begins to be felt at $x/d \cong 500$, but electron-ion recombination is still dominant at $x/d \cong 700$ Because the temperature is dropping along the wake axis, the negative slope of the curve of $n_0 d$ vs x/d in Fig 13 steepens continually Some evidence of this behavior is seen in rounds LL-27 and LL-29, but not in the other two shots This rough calculation illustrates the importance of including the effect of the wake cooling in the analysis By using the scaling parameter λ [Eq (32)], one finds that the conditions represented in Fig 13 correspond to a full-scale body 2 ft in diameter at an altitude of about 143,000 ft Since the geometric scale is increased by a factor of 100, the electron densities in the full-scale wake are 100 times lower than in the wake of the $\frac{1}{4}$-in diam pellet; for example at $x/d = 500$ the full-scale electron density has dropped to a value of about $4\,3 \times 10^7$/cm^3

Recently Labitt[43] measured the decay of electron density in the wakes of small spheres over a six-fold range of ambient pressure Qualitatively, the results indicate a much weaker effect of pressure in the region $n_e < 10^8$/cm^3 than predicted by the simple attachment parameter λ in Eq (32) In fact the electron decay may be much closer to the rate predicted by Eq (24) However, one should probably withhold judgment, in view of the large numerical differences observed in electron density at a given x/d between two different shots at nearly the same velocity and ambient pressure [43] If these experimental difficulties can be overcome, the hypersonic wake may become a useful gasdynamic tool for the study of attachment, detachment, and charge exchange reactions that are important in the ionosphere

5 Problems for Future Research

Wakes behind bodies moving at hypersonic speeds contain most of the modern problems in gas dynamics and some of the ancient ones as well In this paper we have described three interesting areas in which some progress has recently been made But a completely satisfactory description of the hypersonic wake cannot be given until certain gaps in our present knowledge of fluid mechanics, rate processes, and radiation mechanisms are closed In fluid mechanics two of the most challenging problems are: 1) the separated flow just behind the body (Figs 1 and 2), including the "neck"

region; 2) the structure and statistical properties of the turbulent wake

In his original treatment of the "base-flow problem" Chapman[44] dealt with the limiting case of a zero initial boundary-layer thickness; in this case the velocity ratio $u^* = (u/u)\psi_0$ along the dividing streamline takes on the value 0 58 appropriate to free laminar mixing of two unbounded streams If, for example, the enthalpy in the recirculating zone is much lower than the total enthalpy h in the "external" inviscid flow, then the total enthalpy at the stagnation point of the "neck" is also about 0 58 of h (see Ref 2) However the effect of a finite initial boundary-layer thickness cannot be disregarded The work of Denison and Baum,[21] and others,[22, 23] showed that u^* depends on the parameter $(\nu l/\delta^{*2}u)$, where δ^* is the initial displacement thickness and l is distance along the free shear layer But $\delta^{*2} \sim (\nu L/u)$, where L is some appropriate body length, so that u^* is again independent of Reynolds number according to this analysis, and is determined by body shape and Mach number Denison and Baum found values of u^* somewhat lower than Chapman's value of 0 58, but the analysis of Dewey[23] and Kubota shows a strong effect on the value of u^* of the initial velocity profile produced by expansion around the base

Even more important, Dewey's[23] measurements of base pressure on slender, sharp-nosed wedges at $M = 6$ show a definite Reynolds number dependence, amounting to a decrease in base pressure by a factor of about 2 5 when the Reynolds number increases by a factor of 20 Clearly, the influence of the ratio of initial displacement thickness (after expansion) to base height on the recirculation zone must be taken into account; some attempts have been made in this direction [45] The analysis of Reeves and Lees[51] based on integral methods also shows that the interaction between the viscous and inviscid flows during the recompression is an essential part of the problem

Recent measurements of density in the near-wake behind slender bodies in a hypersonic shock tunnel by Zempel and Muntz[46] indicate that the total enthalpy at the neck stagnation point is about 0 3 h In that case the corresponding temperature is about 5400°K at a flight velocity of about 22,000 fps The temperature does not fall much below this value along the laminar wake axis, because laminar diffusion is so slow Thus the laminar portion of the wake is an "incubator" for atoms and electrons This incubation region is terminated by laminar-turbulent transition (Sec 3), because of the rapid cooling along the turbulent portion of the wake Calculations of the production of atoms and electrons in the laminar-wake region have been made by Webb and Hromas[41] and by Pallone[52] using neck temperature as a parameter; they indicate the importance of an accurate determination of the temperature level in the near-wake

Scattering of incident electromagnetic waves by a turbulent wake depends on the scale and intensity of the turbulent fluctuations Once the velocity difference $u_f - u_0$ across the wake becomes subsonic, the turbulence structure should resemble that found by Townsend[12] in the wake behind a cylinder at low speeds Slattery and Clay[7] measured density fluctuations optically in wakes behind spheres, and found some surprisingly large rms values On the basis of these observations, Feldman[47] raises some interesting questions regarding the effect of density and temperature fluctuations on rate processes and equilibrium states

In this paper we have deliberately avoided any discussion of two difficult problems: 1) effect of ablation products deposited in the wake; and 2) radiation from the wake So far as electrons are concerned, if the ablation products form molecular ions, dissociation recombination similar to the $NO^+ + e^-$ reaction may be important [48] If atomic ions are formed they will be much more persistent at high altitudes, because they are removed only by three-body processes Under "normal" conditions electrons contributed by ablation may constitute only a small fraction of the electrons produced naturally in "air," down to altitudes at which oxygen-electron attachment is dominant

Even for pure "air" our understanding of the radiation from hypersonic wakes is still in a primitive state By assuming equilibrium air radiation in the wake of a blunt body, Norling and Kivel[53] of Avco/Everett were able to estimate gas temperatures from experimental measurements of such radiation; the agreement between these estimated temperatures and those calculated by the method of Ref 2 is satisfactory Thompson[49] has also attacked this problem by introducing separate coefficients for absorption and emission, instead of a single gray-body absorption coefficient He has also discussed the nonequilibrium wake radiation problem Of all the observables in the hypersonic wake, radiation is unquestionably the most sensitive to details of chemical composition, temperature, and "impurities"

Clearly, there is no dearth of problems in this rapidly developing field In this situation, close coordination between experimental and theoretical investigations is essential

References

[1] McCarthy, J F, Jr, "Hypersonic wakes," Grad Aeronaut Lab, Calif Inst Tech, Hypersonic Res Project, Memo 67 (July 2, 1962); also McCarthy, J F, Jr and Kubota, T, "A study of wakes behind a circular cylinder at $M = 5$ 7,' AIAA Preprint 63-170 (June 1963)

[2] Lees, L and Hromas, L, "Turbulent diffusion in the wake of a blunt-nosed body at hypersonic speeds," J Aerospace Sci **29**, 976–993 (1962)

[3] Feldman, S, "On trails of axi-symmetric hypersonic blunt bodies flying through the atmosphere, ' J Aerospace Sci **28**, 433–448 (1961)

[4] Vaglio-Laurin, R and Bloom, M, "Chemical effects in external hypersonic flows," *Progress in Astronautics and Rocketry: Hypersonic Flow Research*, edited by F R Riddell (Academic Press Inc, New York, 1962), Vol 7, pp 205–254

[5] Kubota, T, "Laminar wake with streamwise pressure gradient—II," Grad Aeronaut Lab, Calif Inst Tech, Internal Memo 9 (April 1962)

[6] Gold, H, "Laminar wake with streamwise pressure gradient for arbitrary initial velocity and enthalpy distributions," Grad Aeronaut Lab, Calif Inst Tech, Internal Memo 10 (May 1962)

[7] Slattery, R E and Clay, W G, "Width of the turbulent trail behind a hypervelocity sphere," Phys Fluids **4**, 1199–1201 (1961); also "Experimental measurements of turbulent transition, motion, statistics and gross radial growth behind hypervelocity objects, ' Phys Fluids **5**, 849–855 (1962)

[8] Demetriades, A and Gold, H, "Transition to turbulence in the hypersonic wake of blunt-bluff bodies," ARS J **32**, 1420–1421 (1962); also Demetriades, A, "Hot-wire measurements in the hypersonic wake of a cylinder," J Aerospace Sci **28**, 901–902 (1961)

[9] Slattery, R E and Clay, W G, "Reentry physics and project press programs," Semiannual Tech Summary Rept to Advanced Res Projects Agency (U), pp II-11–II-17, Lincoln Lab, Mass Inst Tech (June 30, 1962); also "Laminar-turbulent transition and subsequent motion behind hypervelocity spheres," ARS J **32**, 1427–1429 (1962)

[10] Demetriades, A and Behrens, W, "Hot-wire measurements in the hypersonic wakes of slender bodies," Grad Aeronaut Lab, Calif Inst Tech, Hypersonic Res Project, Internal Memo 14 (May 15, 1963); also Demetriades, A, "Hot wire measurements in the hypersonic wakes of slender bodies," AIAA Preprint 63 444 (August 1963)

[11] Pallone, A J, Erdos, J I, Eckerman, J, and McKay, W, "Hypersonic laminar wakes and transition studies," AIAA Preprint 63-171 (June 1963); also Avco/RAD Tech Memo TM-63-33 (June 14, 1963)

[12] Townsend, A A, *The Structure of Turbulent Shear Flow* (Cambridge University Press, Cambridge, England, 1956), Chap 7

[13] Gibson, W E, 'Dissociation scaling for nonequilibrium blunt nose flows, ' ARS J **32**, 285–287 (1962); also Gibson, W

E and Sowydra, A, "An analysis of nonequilibrium inviscid flows," Cornell Aeronaut Lab Rept AEDC-TDR-62-172 (August 1962)

[14] Hall, J G, Eschenroeder, A Q, and Marrone, P V, "Blunt-nosed inviscid air flows with coupled nonequilibrium process," J Aerospace Sci **29**, 1038–1051 (1962)

[15] Lin, S C and Teare, J D, "A streamtube approximation for calculation of reaction rates in the inviscid flow field of hypersonic objects," Avco Everett Res Lab Res Note 223 (August 1961)

[16] Bloom, M H, "Thermal and chemical effects in wakes," AGARD Meeting on High Temperature Aspects of Hypersonic Flow, Brussels, Belgium (April 1962)

[17] Bloom, M H and Steiger, M H, "Diffusion and chemical relaxation in free mixing," IAS Preprint 63-67 (January 1963)

[18] Lenard, M, Long, M, and Wan, K S, "Chemical nonequilibrium effects in hypersonic pure air wakes," ARS Preprint 2675-62 (November 1962)

[19] Webb, W H and Hromas, L A, "Turbulent diffusion of a reacting gas in the wake of a sharp-nosed body at hypersonic speeds," Space Technology Labs, Inc, Rept 6130 6362-RU-000 (April 15, 1963); also Ballistics Systems Div TDR-63-138 (1963)

[20] Hromas, L and Lees, L, "Effect of nose bluntness on the turbulent hypersonic wake," Space Technology Labs, Inc, Rept 6130-6259 KU-000 (October 1962); also Ballistic Systems Div BSD TDR 62-354 (1962)

[21] Denison, M R and Baum, E, "Compressible free shear layer with finite initial thickness," IAS Paper 62-125 (June 1962); also AIAA J **1**, 342–349 (1963)

[22] Hammitt, A G, "Effects of the separated region on the heat transfer and flow about a chin radome configuration," General Applied Science Lab Rept 14 (November 1959)

[23] Dewey, C F, Jr, "Measurements in highly dissipative regions of hypersonic flows Part II," Ph D Thesis, Calif Inst Tech, Pasadena, Calif (1963)

[24] Chapman, D R, Kuehn, D M, and Larson, H K, "Investigation of separated flows in supersonic and subsonic streams with emphasis on the effect of transition," NACA Rept 1356 (1958)

[25] Larson, H K, "Heat transfer in separated flows," J Aerospace Sci **26**, 731–738 (1959); also Larson, H K and Keating, S J, Jr, "Transition Reynolds numbers of separated flows at supersonic speeds," NASA TN D-439 (December 1960)

[26] Stetson, K F, "Boundary layer transition on blunt bodies with highly cooled boundary layers," J Aerospace Sci **27**, 81–90 (1960)

[27] Lin, C C, "On the stability of the laminar mixing region between two parallel streams in a gas," NACA TN 2887 (1953)

[28] Lees, L and Lin, C C, "Investigation of the stability of a laminar boundary layer in a compressible fluid," NACA TN 1115 (1946)

[29] Lees, L, "Stability of the laminar boundary layer in a compressible fluid," NACA TR 876 (1947)

[30] Landau, L, "Stability of tangential discontinuities in compressible fluid," Compt Rend Acad Bulgare Sci **XLIV**, 139–141 (1944)

[31] Webb, M, Hromas, L, and Lees, L, "Remarks on hypersonic wake transition," Space Technology Labs, Inc, Rept 6130-6360-KU-000 (September 1962); also AIAA J **1**, 719–720 (1963)

[32] Gold, H, "Stability of laminar wakes," Ph D Thesis, Calif Inst Tech, Pasadena, Calif (1963)

[33] Batchelor, G K and Gill, A E, "Analysis of the stability of axi-symmetric jets," J Fluid Mech **14**, 557–567 (1962)

[34] Sato, H and Kuriki, K, "The mechanism of transition in the wake of a thin flat plate placed parallel to a uniform flow," J Fluid Mech **11**, 321–352 (1961)

[35] Kendall, J M, Jr, "Experimental study of cylinder and sphere wakes at a Mach number of 3 7," Jet Propulsion Lab, Calif Inst Tech, TR 32-367 (November 13, 1962)

[36] Lin, S C, "Radio echoes from a manned satellite during reentry," J Geophys Res **62**, 3851–3870 (1962)

[37] Hammerling, P, Teare, J D, and Kivel, B, "Nonequilibrium electrical and radiative properties of high temperature air, nitrogen, and oxygen," *Proceedings of the 4th International Conference on Ionization Phenomena in Gases* (North Holland Publishing Co, Amsterdam, Holland, 1960), pp 1092–1097

[38] Eschenroeder, A Q, Daiber, J W, Golian, T. C, and Hertzberg, A, "Shock tunnel studies of high-enthalpy ionized airflows," Cornell Aeronaut Lab Rept AF-1500-A-1 (July 1962)

[39] Chanin, L M, Phelps, A V, and Biondi, M A, "Measurement of the attachment of slow electrons in oxygen," Phys Rev Letters **2**, 344–346 (1959)

[40] Phelps, A V and Pack, J L, "Collisional detachment in molecular oxygen," Phys Rev Letters **6**, 111–113 (1961)

[41] Webb, W H and Hromas, L A, 'Turbulent diffusion of a reacting wake," AIAA Preprint 64-42 (January 1964)

[42] Labitt, M and Herlin, M A, "Electron density measurements in the wakes of hypervelocity pellets,' Mass Inst Tech, Lincoln Lab Rept 35G-002 (May 25, 1961)

[43] Labitt, M, "The measurement of electron density in the wake of a hypervelocity pellet over a six-magnitude range," Mass Inst Tech, Lincoln Lab TR 307 (April 15, 1963)

[44] Chapman, D R, "An analysis of base pressure at supersonic velocities and comparison with experiment," NACA Rept 1051 (1951); supersedes NACA TN 2137 (1950)

[45] Rom (Rabinowicz), J, "Theory for supersonic two-dimensional laminar base-type flows using the Crocco-Lees mixing concepts," J Aerospace Sci **29**, 963–968 (1962)

[46] Zempel, R E and Muntz, E P, "Slender body near-wake density measurements at Mach numbers 13 and 18," AIAA Preprint 63-271 (June 1963)

[47] Feldman, S, "A problem in turbulent reacting gas dynamics," Anti-Missile Res Advisory Committee Proc **VI**, 233 (April–May 1962)

[48] Eschenroeder, A Q, "Ionization nonequilibrium in expanding flows," ARS J **32**, 196–203 (1962)

[49] Thompson, T R, "The gray gas in hypersonic flow," Ae E Thesis, Calif Inst Tech, Pasadena, Calif (1963)

[50] Behrens, W, unpublished data, Grad Aeronaut Lab, Calif Inst Tech (1963)

[51] Reeves, B and Lees, L, "Supersonic separated and reattaching laminar flows: general theory and application to adiabatic boundary layer shock wave interactions," AIAA Preprint 64-4 (January 1964)

[52] Pallone, A, private communication (1963)

[53] Norling, R A and Kivel, B, private communication (1963)